The Little Ice Age and Medieval Warm Period in the Sargasso Sea

Lloyd D. Keigwin

The Little Ice Age and Medieval Warm Period in the Sargasso Sea

Lloyd D. Keigwin

Sea surface temperature (SST), salinity, and flux of terrigenous material oscillated on millennial time scales in the Pleistocene North Atlantic, but there are few records of Holocene variability. Because of high rates of sediment accumulation, Holocene oscillations are well documented in the northern Sargasso Sea. Results from a radiocarbon-dated box core show that SST was ~1°C cooler than today ~400 years ago (the Little Ice Age) and 1700 years ago, and ~1°C warmer than today 1000 years ago (the Medieval Warm Period). Thus, at least some of the warming since the Little Ice Age appears to be part of a natural oscillation.

With the exception of nearshore anoxic basins (1), climate data from marine sediments generally lack sufficient time resolution to be compared directly to instrumental observations. Thus, there has been a gap in our knowledge of the ocean-climate system between the millennial-scale climate changes resolved in the best sediment cores from the open ocean and decadal scale changes observed in instrumental data. This gap occurs on the century time scale, the very time scale on which anthropogenic warming is thought to be occurring (2). Hence, it is important to document natural climate variability in order to understand the effects of anthropogenic forcing. Here I report on the record of climate change for the past few millennia from the Bermuda Rise in the northern Sargasso Sea, a location where century-scale resolution is possible.

The Bermuda Rise is a remarkable archive of proxy climate information. Rates of sediment accumulation as high as 200 cm per thousand years are maintained by deep recirculating gyres (3) which focus detrital silt and clay at this locale (4). Cycles of various sedimentary properties occurred in the late Pleistocene with a quasi period of 4000 years (5), extending through the latest deglaciation and into the Holocene (6). In the late Pleistocene these variations are found in calcium carbonate content, in stable isotope ratios of oxygen and carbon, and in Cd/Ca ratios, all of which are thought to reflect, in part, changes in SST and changes in the production of North Atlantic Deep Water. Sampling of the last ~10,000 years (the Holocene) on the Bermuda Rise had not been sufficient to determine precisely the state of the modern climate system with respect to these millennial-scale cycles.

To address this question, I studied a box core (HU89038 BC-004) taken from the same location as previous cores (7).

Piston core KNR31 GPC5 has a reservoir-corrected accelerator mass spectrometer (AMS) ^{14}C age of 860 years at the top (6). In contrast, each of two sub cores (A and B) of BC-004 has zero or negative planktonic foraminiferal ages after reservoir correction (Fig. 1, A and B, and Table 1). This age difference must result from better recovery of the sediment surface by BC-004. Zero or negative ages reflect excess ^{14}C produced by atmospheric nuclear weapons testing and attest to the high deposition rates at this site because the signal has not been diluted on the seafloor by upward mixing of older foraminifera. Additional AMS ^{14}C measurements at each subcore of BC-004 have been used to develop an age model (Fig. 1C) for stacking the data (Fig. 1F) (8). Evidently piston core GPC-5 failed to recover the uppermost ~15 cm of the seafloor at this location.

Percent CaCO$_3$ near the top of the box core decreases from maximum values between ~1000 and 500 years ago to the most pronounced minimum of the past 10,000 years, centered on ~400 years ago (Figs. 1F and 2). This minimum and the preceding maximum are equivalent in age to the climate events loosely known as the Little Ice Age (LIA) and the Medieval Warm Period (MWP), respectively (9). Together with the slight increase in carbonate in the upper few centimeters of the core, the minimum and maximum define the third of three cycles during the last 5000 years on the Bermuda Rise. This broad interval is often referred to as the period of Neoglaciation (10), which followed an early Holocene period of warmer climate (the Hypsithermal; Fig. 2). It is

Table 1. Results of accelerator mass spectrometer radiocarbon dating of Bermuda Rise box core HU89-038-BC4 at the National Ocean Sciences Accelerator Mass Spectrometer Facility, Woods Hole, Massachusetts. All ages in years before present.

Depth (cm)	No.	Fraction modern	Measured age	Reservoir corrected age	Calendar age†	Calendar age range, ±1σ
			HU89-038-BC 004A			
0.5	311	0.9501	410 ± 80	10	0	0
0.5	313	1.0220	–	0	0	0
0.5	315	0.9608	320 ± 150	0	0	0
4.5	2984	0.9036	815 ± 40	415	455	424–481
9.5	2985	0.9053	800 ± 40	400	443	416–469
10.5	5328	0.8786	1040 ± 60	640	619	549–647
13.5	5329	0.8490	1310 ± 40	910	866	795–899
17.5	2981	0.8324	1470 ± 40	1070	989	951–1047
23.5	2982	0.8165	1630 ± 45	1230	1177	1135–1235
29.5	2983	0.8091	1700 ± 40	1300	1254	1220–1279
32.5	2978	0.7472	2340 ± 70	1940	1937	1861–2020
38.5	2979	0.6991	2880 ± 40	2480	2689	2643–2721
44.5	2980	0.6778	3120 ± 40	2720	2867	2827–2929
			HU89-038-BC 004D			
0.5	5178	0.9513	400 ± 40	0	0	0
1.5	5321	0.9665	275 ± 30	0	0	0
2.5	5176	1.0540	–	0	0	0
3.5	5177	0.9855	115 ± 30	0	0	0
4.5	5322	0.9587	340 ± 30	0	0	0
5.5	5172	0.9080	775 ± 40	375	424	385–452
6.5	5319	0.8982	860 ± 40	460	483	461–503
7.5	5171	0.8963	880 ± 30	480	494	475–510
8.5	5323	0.9003	845 ± 20	445	474	457–490
10.5	5324	0.9034	815 ± 40	415	455	428–478
13.5	5320	0.8585	1230 ± 20	830	749	723–777
45.5	5325	0.6921	2960 ± 30	2560	2731	2714–2747
48.5	5326	0.6633	3300 ± 30	2900	3129	3077–3177
50.5	5327	0.6669	3250 ± 40	2850	3059	2984–3115

*Corrected by −400 years for the age of the surface ocean reservoir.   †Calendar ages have been calibrated according to (26).

Woods Hole Oceanographic Institution, Woods Hole, MA 02543 USA.

likely that carbonate flux was relatively constant and the flux of terrigenous sediment delivered to the Bermuda Rise by deep currents increased during the LIA, just as it did during earlier carbonate minima in the Holocene and during glaciation (4). For both the LIA and the carbonate minimum of ~1300 years ago, increased flux of terrigenous clay and silt particles probably accounts for the significant increases in sedimentation rates indicated by the AMS dates (Fig. 1C). This terrigenous sediment most likely was resuspended from the Scotian Rise during abyssal storms (11), or eroded from the northeast scarp of the Bermuda Rise (12). Atmospheric storminess could force the Gulf Stream to be more energetic, in turn increasing the kinetic energy of the deep recirculating gyres to which it is linked (13). Historical evidence (14) and geological evidence at nearshore locations (15) point to increased storminess during the LIA in the North Atlantic region.

Whether the source of the terrigenous dilutant was local (Bermuda Rise scarp) or more distal (Scotian Rise), the prevailing deep flow would transport this sediment to the plateau of the Bermuda Rise (3). At present, the geochemical evidence for changes in NADW production is ambiguous, so it is not known if there was actually a change in the source of deep waters associated with the LIA, as there was for similar events in the Pleistocene (5, 16). In general, it is thought that any Holocene changes in deep ocean water masses were small compared to those during deglacial and older times (17).

Oxygen isotope ratios (δ^{18}O) are a more direct proxy for climate change during the late Holocene in the Sargasso Sea than percent carbonate. For isotopic analysis I chose the planktonic foraminifera *Globigerinoides ruber* (white variety, 150 to 250 μm). The white variety of this species lives year-round in the upper 25 m of the northern Sargasso Sea and has a relatively constant annual mass flux and shell flux (18). Thus, of all planktonic foraminifera at this location this species is most appropriate for reconstructing annual average SSTs (18).

Oxygen isotopic variations of *G. ruber* in BC-004 should represent only the influence of SST and salinity variations in the Sargasso Sea. Results at each subcore generally vary in concert with the percent $CaCO_3$. Maximum δ^{18}O values are associated with minimum percent $CaCO_3$ (Fig. 1, D and E) as they are earlier in the Holocene (Fig. 2). Increased δ^{18}O and decreased percent $CaCO_3$ are consistent with climatic cooling in the Pleistocene on the Bermuda Rise (5) and at other

North Atlantic locations. At times, the δ^{18}O results show even higher frequency variability than that of the carbonate record, especially during the uppermost maximum in percent $CaCO_3$ (Fig. 1, D and E). Along with evidence of slightly different phasing between the carbonate and δ^{18}O records in the Pleistocene (5), unlinking of the two by just ~1000 years ago suggests that the δ^{18}O results are not an artifact of carbonate dissolution. The occurrence of identical oscillations of

δ^{18}O values in *G. ruber* and the solution-resistant *Globorotalia inflata* at this location during the prolonged deglacial carbonate minimum provides additional evidence that *G. ruber* is recording a primary surface water signal (6).

The 42-year series of hydrographic data at Bermuda Station "S", which is ~700 km to the southwest of BC-004, provides an important baseline for interpreting the geological record because within this broad region hydrographic properties show
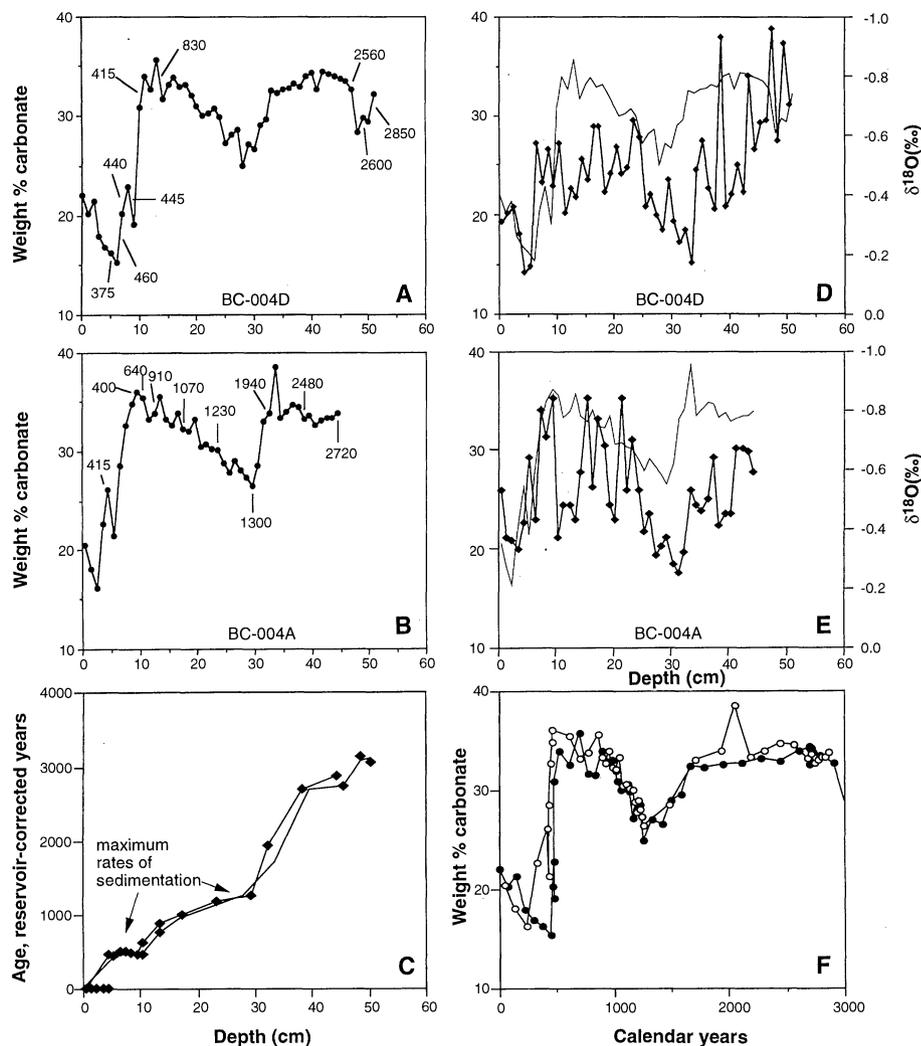

Fig. 1. Sedimentological, oxygen isotopic, and radiocarbon data on Bermuda Rise core HU89038 BC-004. (**A** and **B**) Weight percent carbonate in two subcores of BC-004 with results of AMS ^{14}C dating on mixed planktonic foraminifera (see Table 1). The radiocarbon dates have been corrected by −400 years to account for the age of surface waters in which the foraminifera grew. Dates near the core top with zero or negative ages after reservoir correction are not shown. One ^{14}C analysis in each subcore gave a fraction of modern carbon >1, indicating that the negative ages reflect the presence of bomb ^{14}C. (**C**) Age-depth plots for the two subcores showing the age models adopted for stacking the data. Note that the highest rates of sedimentation occur where percent carbonate is a minimum, supporting the interpretation that dilution by clay and silt particles drives the percent carbonate results. (**D** and **E**) Oxygen isotope results on the surface-dwelling planktonic foraminifera *G. ruber* (diamonds) overlying the carbonate results (thin lines). Occasional samples were analyzed in duplicate, including the isotopically light points between 35 and 50 cm in (D). (**F**) Percent carbonate results on a calendar-year age model based on the control points in (C). Open symbols, BC-004A; solid symbols, BC-004D.

little geographic variability (*19, 20*). Interdecadal variability in monthly normalized property anomalies are well known at Station "S" (*19–22*), but even on an annual average basis a major event like the late 1960s decrease in SST and increase in salinity stands out (Fig. 3) (*23*). That climatic extreme and similar episodes at other times are associated with minima in the North Atlantic Oscillation, strong westerlies at lower middle latitudes (*24*), and southwestward movement of storm centers in the North Atlantic (*25*).

In order to gauge the influence of the annual variability of SST and salinity on the oxygen isotope ratios that might be recorded by surface-dwelling planktonic foraminfera at Station "S", I calculated the $\delta^{18}O$ value of calcite precipitated in oxygen isotopic equilibrium with seawater (Fig. 3) (*26*). As expected, the effects of decreased SST and increased salinity during the late 1960s combined to increase the $\delta^{18}O$ value of equilibrium calcite. Over the full 42-year series, linear regressions between the SST, salinity, and $\delta^{18}O$ values show that temperature accounts for about two-thirds of the isotopic signal ($r^2 = 0.61$), whereas salinity accounts for one-third ($r^2 = 0.29$). Thus, by comparison to sea surface changes during the past several decades, it is reasonable to interpret the

foraminiferal isotopic data mostly in terms of SST change.

When the $\delta^{18}O$ data from each subcore are plotted together on a calendar time scale (*27*), it is clear that the same features are present in each subcore (*28*). Within each subcore $\delta^{18}O$ values reach a minimum ~500, 900, and 1100 years ago (Fig. 4A). Using these data, I solved the paleotemperature equation (*26*) after applying Deuser's disequilibrium correction (*18*) of +0.2 per mil to the $\delta^{18}O$ value of G. *ruber* and assuming that the average salinity was 36.5 per mil. I then stacked the temperature proxy data from the two subcores by averaging results in 50-year bins (Fig. 4B). In general, these results indicate that there have been century-scale changes in SST of 1° to 2°C throughout the past few thousand years in the Sargasso Sea. In the last half of the record there was a 1.5°C oscillation from a minimum SST 1500 to 1700 years ago to a maximum 900 to 1000 years ago, to a minimum 300 to 400 years ago. Since the Little Ice Age, SSTs in the northern Sargasso Sea increased by ~1°C. Actual SST changes may have been even greater than indicated in Fig. 4B, in that the sediment may have been mixed differentially by burrowing (~5 cm) as sedimentation rates changed, and because stacking the $\delta^{18}O$ data may have attenuated the signal. From the raw $\delta^{18}O$ data of BC-004D (Fig. 4A), calculated SST 350 years ago was 21.5°C, about 1.5°C colder than the modern annual average.

Depression of SSTs by 1° to 2°C during the LIA is consistent with other proxy data from the Sargasso Sea region and is probably part of a much larger climatic pattern (*29*). The 800-year record of coral growth near Bermuda has been interpreted in terms of SST cooling of this magnitude, which was induced at least in part by wind-driven vertical mixing and heat flux changes (*30*). Far to the west in the Florida Strait, $\Delta^{14}C$ and $\delta^{18}O$ values on coral also indicated that SSTs were lower by 1° to 2°C between ~A.D. 1680 and 1750 during the LIA (*31*).

Abrupt, century-scale changes in SSTs in the Sargasso Sea may have influenced climate downstream in widespread regions to the east. It is thought that SST changes in the North Atlantic (as well as global changes) induce changes in African rainfall (*32*), and the lake level history of tropical African Lake Bosumtwi indicates that extended drought and lowest lake levels in the Holocene occurred during the LIA (*33*). Summer temperature estimates derived from tree rings in northern Fennoscandia show that the MWP consisted of two events, the first in the 10th and 11th centuries and the second in the

Fig. 2. Holocene climate proxy data from the Bermuda Rise, northern Sargasso Sea. (**Top**) Oxygen isotope ratio of the surface-dwelling planktonic foraminifera G. *ruber* from BC-004 and nearby gravity core EN120 GGC-1. The box core data are a stack of the data in Fig. 4A at 1-cm spacing, and the gravity core data are at 2-cm spacing. Where the two cores overlap, the GGC-1 data were added to the box core stack. Because of the different sampling intervals between the two cores and the increasing rate of sedimentation since the early Holocene minimum (*6*), data for the last 3000 years have higher resolution. (**Bottom**) Percent carbonate results from core GPC-5 (solid circles), GGC-1 (open circles), and BC-004 (triangles). Note that the three major carbonate minima (~3500, ~1500, and ~400 years ago) are closely matched by oxygen isotopic maxima (top panel) but that the isotopic data also contain a higher frequency signal.
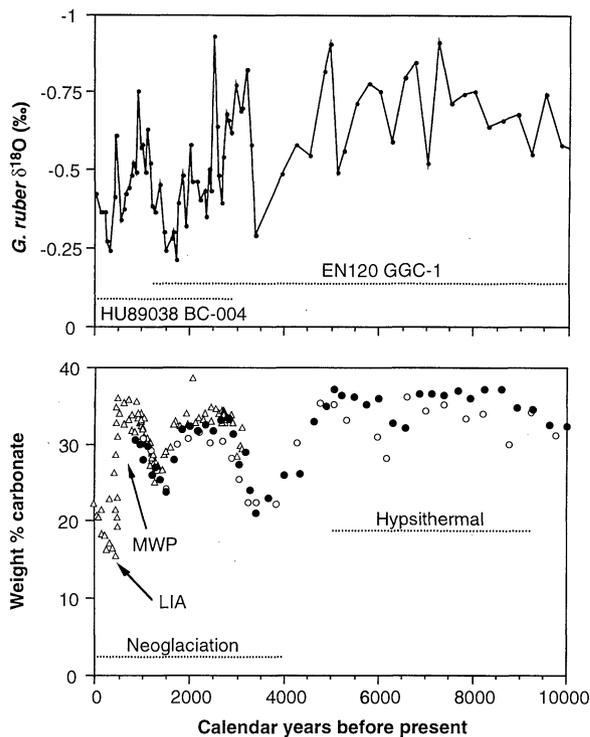

Fig. 3. Annual average data from Station "S," near Bermuda (32° 10'N, 62°30'W). The temperature and salinity data are scaled in proportion to their effect on the $\delta^{18}O$ of calcite precipitated in equilibrium with seawater (solid data) to show that the temperature effect on $\delta^{18}O$ is about twice that of the salinity effect over recent decades at this location. Note that unlike most locations the temperature and salinity from this part of the Sargasso Sea are only slightly correlated (or not at all). However, during a pronounced climate event like the minimum in the North Atlantic Oscillation of the late 1960s, the SST and salinity combine to produce a robust increase in $\delta^{18}O$ values.
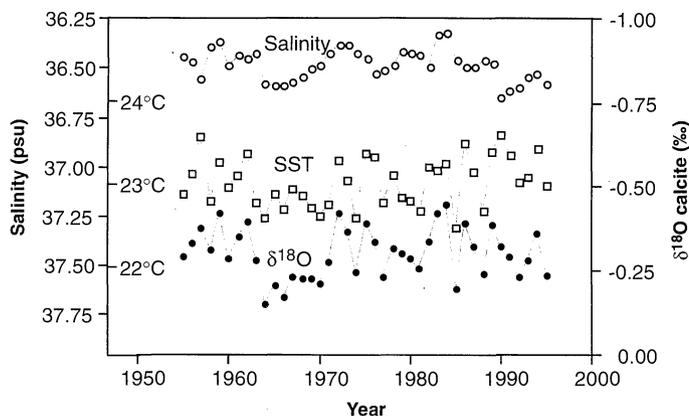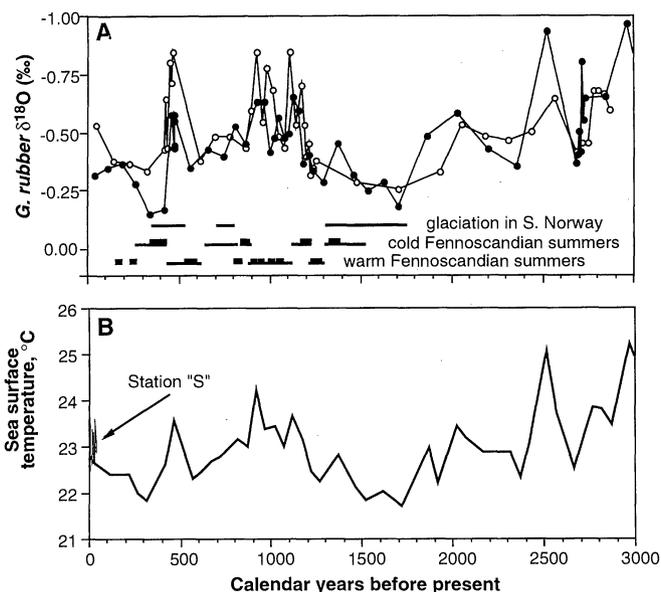
early 15th century (34). Furthermore, these are bracketed by cold events (34) that seem to correlate with glacier expansion in southern Norway (35). During the LIA, glaciers in southern Norway reached their greatest extent of the past 9000 years (35). Thus, as is summarized in Fig. 4A, it appears that the high-resolution SST record from the Bermuda Rise is consistent with the multidecadal trends in the highest resolution records of climate proxy data on land to the east.

Over the course of three millennia, the range of SST variability in the Sargasso Sea is on the order of twice that measured over recent decades (Fig. 4B). Increased variance of climatic spectra on longer time scales has been demonstrated for the climate system in general (36), and for the North Atlantic region in particular (37). Although forcing for climate change on millennial and centennial time scales is still poorly understood, the North Atlantic Oscillation (NAO) may provide a useful model for interpreting long-term SST changes in the western Sargasso Sea. If NAO minimum conditions were more persistent during the LIA they could account for many of the Bermuda Rise observations and the coral observations, including SST depression, salinity increase, increased pumping of nutrients to the sea surface (increasing coral growth rates), and increased terrigenous load in deep recirculating gyres as a result of the south-

westward shift in storm tracks. Dickson et al. (22) concluded that on interdecadal (NAO) time scales convection in the Sargasso Sea (formation of subtropical mode water) is in phase with convection in the Greenland Sea, and out of phase with convection in the Labrador Sea. This pattern is similar to the sort of convective dipole that has been proposed to operate on glacial-interglacial time scales (38) in order to account for the change from deep to intermediate depth ventilation in the North Atlantic (17, 39). It would be interesting to know if the same style of climate and ocean variability occurs in the North Atlantic across the full spectrum of 10^1 to 10^5 years.

Because climate events like the LIA and MWP were of long enough duration (decades to centuries) to be resolved in Bermuda Rise sediments, and because the changes described here for surface waters over the Bermuda Rise are probably typical of a large part of the western Sargasso Sea, they most likely reflect climate change on the basin or hemispheric scale. Regardless of the exact cause for the LIA, the MWP, and earlier oscillations, the warming during the 20th century (0.5°C) (2) is not unprecedented. However, it is important to distinguish natural climate change from anthropogenic effects because human influence may be occurring at a time when the climate system is on the warming limb of a natural cycle.

REFERENCES AND NOTES

1. N. G. Pisias, Quat. Res. 10, 66 (1978); A. Juillet-Leclerc and H. Schrader, Nature 329, 146 (1987); J. P. Kennett and B. L. Ingram, ibid. 377, 510 (1995); K. A. Hughen, J. T. Overpeck, L. C. Peterson, S. Trumbore, ibid. 380, 51 (1996).
2. P. D. Jones, T. M. L. Wigley, P. B. Wright, Nature 322, 430 (1986); B. D. Santer et al., Clim. Dynam. 12, 77 (1995); B. D. Santer et al., Nature 382, 39 (1996).
3. E. P. Laine and C. D. Hollister, Mar. Geol. 39, 277 (1981); W. J. McCartney and M. S. McCartney, Rev. Geophys. 31, 29 (1993).
4. M. P. Bacon and J. N. Rosholt, Geochim. Cosmochim. Acta 46, 651 (1982); D. O. Suman and M. P. Bacon, Deep-Sea Res. 36, 869 (1989).
5. L. D. Keigwin and G. A. Jones, J. Geophys. Res. 99, 12397 (1994).
6. ——, Deep-Sea Res. 36, 845 (1989).
7. BC-004 was recovered from 33°41.6'N, 57°36.7'W by CSS Hudson at 4418 m on the undulating plateau of the northeast Bermuda Rise, within 1000 m of KNR31 GPC-5 (6) and EN120 GGC1 (17). The box core was subcored using plastic pipe with a diameter of 11.4 cm.
8. As BC-004A is generally better dated than BC-004D, the two were correlated and ages assigned to the latter to bring the carbonate curves into line (Fig. 1F). For the last 500 years, BC-004D is more intensely dated, and an age model was chosen for the interval from 5.5 to 10.5 cm to be within the 1σ age errors (Table 1). Although the age of the youngest carbonate minimum differs slightly between the two subcores, the age model brings δ^{18}O results into good agreement (Fig. 4A).
9. In this report these names are used informally to denote cooling several hundred years ago, and warming about 1000 years ago. Although there is general agreement that there was cooling and glacial expansion in many regions during the LIA interval, and warming during the MWP interval, it is by no means certain that specific events or even these intervals were synchronous and worldwide. Contrast, for example, M. K. Hughes and H. F. Diaz, Clim. Change 26, 109 (1994) with J. M. Grove and R. Switsur, ibid. 26, 143 (1994). See also R. S. Bradley and P. D. Jones, Climate Since A.D. 1500 (Routledge, London, 1995).
10. S. C. Porter and G. H. Denton, Am. J. Sci. 265, 177 (1967).
11. Brief events of intense deep current activity and sediment resuspension known as abyssal storms have been observed off Nova Scotia by C. D. Hollister and I. N. McCave [Nature 309, 220 (1994)].
12. E. P. Laine, W. D. Gardner, M. J. Richardson, M. Kominz, Mar. Geol. 119, 159 (1994).
13. L. V. Worthington, On the North Atlantic Circulation. (Johns Hopkins Oceanogr. Stud. 6, Johns Hopkins University, Baltimore, 1976).
14. H. H. Lamb, Quat. Res. 11, 1 (1979).
15. H. C. Hass, Mar. Geol. 111, 361 (1993); D. J. W. Piper, M. Feetham, J. Goulden, paper presented at the Fifth International Conference on Paleoceanography, Halifax, Nova Scotia, 10 to 14 October 1995, p. 58.
16. E. A. Boyle and P. D. Rosener, Palaeogeogr. Palaeoclimatol. Palaececol. 89, 113 (1990); D. W. Oppo and S. J. Lehman, Paleoceanography 10, 901 (1995).
17. E. A. Boyle and L. D. Keigwin, Nature 330, 35 (1987).
18. W. G. Deuser, J. Foraminiferal Res. 17, 14 (1987).
19. L. D. Talley, Physica D, in press.
20. T. M. Joyce and P. Robbins, J. Clim., in press.
21. L. D. Talley and M. E. Raymer, J. Mar. Res. 40 (suppl.), 757 (1982); W. J. Jenkins, ibid., p. 265.
22. R. Dickson, J. Lazier, J. Meincke, P. Rhines, Prog. Oceanogr., in press.
23. This part of the Sargasso Sea is unlike most other locations in that surface temperature and salinity are not significantly correlated (19, 20). This probably results from latent heat loss associated with storminess [(19); see also (24)]. Joyce and Robbins (20) also point out the contribution of summer rains which begin near Bermuda after establishment of the seasonal thermocline. With regards to the δ^{18}O values,

Fig. 4. (A) Oxygen isotope ratios of the surface dwelling planktonic foraminifera *G. ruber* from Bermuda Rise BC-004 plotted versus calendar age. Open symbols, BC-004A; solid symbols, BC-004D. Bars above the abcissa are a schematic representation of proxy data for episodes of glacial expansion in southern Norway (35) and summer temperature variability in Fennoscandia reconstructed from tree rings (34). For the tree ring data, temperature maxima and minima are shown by thicker bars. For the glacier data, the bars represent two early periods of expansion (but not to LIA limits), followed by the range of age estimates for attainment of the LIA maximum (35). These terrestrial data, which are downstream of the North Atlantic, are generally consistent with the δ^{18}O data (maxima correspond to cooling; minima to warming). **(B)** Sea surface temperatures calculated from the δ^{18}O data in (A), after averaging the data in 50-year intervals, plotted with the annual average of SST measured at Station "S" since 1954 (from Fig. 3). Although, as discussed in the text, about one-third of SST variability calculated from δ^{18}O values (before stacking) may actually reflect salinity change in the Sargasso Sea, it is clear that on centennial and millennial time scales, SST variability has been greater than has been measured over the past four decades at Station "S."

the influences of temperature and salinity changes in the Sargasso Sea surface are additive, whereas they tend to cancel each other at other locations.

24. D. R. Cayan, *J. Clim.* **5**, 354 (1992); Y. Kushnir, *ibid.* **7**, 141 (1994).
25. R. R. Dickson and J. Namias, *Mon. Weather Rev.* **104**, 1255 (1976).
26. Equilibrium calcite precipitation was calculated using annual average Station "S" data, the North Atlantic salinity-$\delta^{18}O$ relationship [H. Craig and L. I. Gordon, *Symposium on Marine Geochemistry* (*Occas. Publ. 3*, Narragansett Marine Laboratory, Naragansett, RI, 1965)], and Shackleton's paleotemperature equation [N. J. Shackleton, *CNRS Colloq.* **219**, 203 (1974)].
27. Using the calibration of M. Stuiver and P. J. Reimer, *Radiocarbon* **35**, 215 (1993).
28. Subcores A and D were analyzed on two different mass spectrometers (a VG Prism and a partially automated VG Micromass 903, respectively). Although there might be a slight intercalibration difference be-

tween the two instruments, the small differences among the $\delta^{18}O$ results most likely reflect sedimentary processes such as bioturbation. All data are archived at the NOAA/NGDC World Data Center-A for Paleoclimatology (paleo@mail.ngdc.noaa.gov).
29. R. S. Bradley and P. D. Jones, *Holocene* **3**, 367 (1993).
30. J. Patzold and G. Wefer, paper presented at the *Fourth International Conference on Paleoceanography*, Kiel, p. 224 (1992); R. B. Dunbar and J. E. Cole, *Coral Records of Ocean-Atmosphere Variability* (University Corporation for Atmospheric Research, Boulder, CO, 1993).
31. E. M. Druffel, *Science* **218**, 13 (1982).
32. C. K. Folland, T. N. Palmer, D. E. Parker, *Nature* **320**, 602 (1986).
33. M. R. Talbot and G. Delibrias, *ibid.* **268**, 722 (1977); *Earth Planet. Sci. Lett.* **47**, 336 (1980).
34. K. R. Briffa *et al.*, *Nature* **346**, 434 (1990); *Clim. Dynam.* **7**, 111 (1992).

35. J. A. Matthews, *Holocene* **1**, 219 (1991).
36. J. M. Mitchell Jr., *Quat. Res.* **6**, 481 (1976).
37. J. E. Kutzbach and R. A. Bryson, *J. Atmos. Sci.* **31**, 1958 (1974).
38. S. J. Lehman and L. D. Keigwin, *Nature* **358**, 198 (1992).
39. D. W. Oppo and S. J. Lehman, *Science* **259**, 1148 (1993).
40. I thank C. E. Franks and E. Roosen for technical assistance; R. Bradley, E. Druffel, and R. Dunbar for comments on the manuscript; M. McCartney, T. Joyce, W. Schmitz, E. Boyle, S. Lehman, and W. Jenkins for discussions; and I. Hardy, K. Moran, and the Bedford Institute of Oceanography for help in acquiring and archiving BC-004. This work was funded by the NOAA Atlantic Climate Change Program.

A Combined Experimental and Theoretical Study on the Formation of Interstellar C₃H Isomers
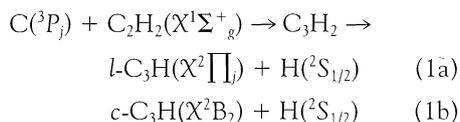
R. I. Kaiser, C. Ochsenfeld, M. Head-Gordon, Y. T. Lee, A. G. Suits

The reaction of ground-state carbon atoms with acetylene was studied under single-collision conditions in crossed beam experiments to investigate the chemical dynamics of forming cyclic and linear C₃H isomers (c-C₃H and l-C₃H, respectively) in interstellar environments via an atom-neutral reaction. Combined state-of-the-art ab initio calculations and experimental identification of the carbon-hydrogen exchange channel to both isomers classify this reaction as an important alternative to ion-molecule encounters to synthesize C₃H radicals in the interstellar medium. These findings strongly correlate with astronomical observations and explain a higher [c-C₃H]/[l-C₃H] ratio in the dark cloud TMC-1 than in the carbon star IRC+10216.

For more than two decades, networks of radiative association, dissociative recombination, and exothermic ion-molecule reactions have been postulated to account for chemistry in the interstellar medium (ISM) (*1*). Such reactions involve ubiquitous radicals such as linear and cyclic C₃H (l-C₃H, propynylidyne, and c-C₃H, cyclopropynylidene) (*2*); for example, addition of C^+ to C_2H_2 yielding l/c-C_3H^+ + H is thought to be followed by a subsequent radiative association of l/c-C_3H^+ and H_2 to c-$C_3H_3^+$, and a final dissociative electron-ion recombination forming l/c-C_3H and two hydrogen atoms or H_2. This framework, however, cannot reproduce observed number densities and isomer ratios. Fueled by recent kinetic studies of barrierless, fast neutral-neutral reactions of atomic carbon $C(^3P_j)$ with unsaturated hydrocarbons (*3*), Herbst and co-workers implemented this reaction class into generic models of the dark molecular cloud

TMC-1 and the circumstellar envelope surrounding the carbon star IRC+10216 to improve the fit to astronomical surveys (*4*). These models, however, suffer from sparse laboratory data on reaction products and cannot elucidate the contribution to distinct structural isomers such as l/c-C₃H. Therefore, even this refined network does not explain the interstellar c-C₃H to l-C₃H ratio of unity in cold molecular clouds compared to 0.2 ± 0.1 around IRC+10216. Hence the formation of interstellar C₃H isomers remains to be resolved.

In this report, we present combined high-level ab initio calculations and crossed-beam experiments on the atom-neutral reaction 1 to interstellar C₃H isomers via C₃H₂ intermediates:

$$C(^3P_j) + C_2H_2(X^1\Sigma_g^+) \rightarrow C_3H_2 \rightarrow$$

$$l\text{-}C_3H(X^2\textstyle\prod_j) + H(^2S_{1/2}) \qquad (1a)$$

$$c\text{-}C_3H(X^2B_2) + H(^2S_{1/2}) \qquad (1b)$$

This system represents the prototype reaction of ubiquitous interstellar carbon atoms with the simplest unsaturated hydrocarbon

molecule, acetylene, to synthesize hydrocarbon radicals via a single atom-neutral collision in interstellar environments. The circumstellar shell of IRC+10216, for example, contains C_2H_2 as well as $C(^3P_j)$ reservoirs at distances of 10^{14} to 10^{15} m from the central star (*5*), and formation of C_3H via reaction 1 is feasible. Our investigations also provide dynamical information on the elementary steps to C₃H isomers. The laboratory data strongly depend on the structures of the initially formed C₃H₂ collision complexes, and therefore we first calculated the ab initio geometries of energetically accessible C₃H₂ isomers. We then compared our crossed-beam data and experimental dynamics with those arising from distinct C₃H₂ adducts. Once the isomers were identified, we determined the exit channels from C₃H₂ following a carbon-hydrogen bond rupture to c-C₃H, or l-C₃H, or both.

Ab initio electronic structure calculations were performed at a level of theory high enough to predict relative energies of all local minima and reaction exothermicities to a precision of about 1 to 3 kJ mol^{-1} (*6*). The discussion is limited to the triplet potential energy surface (PES) because no triplet C₃H₂ minimum fulfills the requirements for intersystem crossing (*7*). Our ab initio calculations show that propargylene, HCCCH, is the global minimum on the triplet C₃H₂ PES and is bound by 385.4 kJ mol^{-1} with respect to the reactants (Fig. 1 and Table 1). The structure has an almost linear C–C–C angle of 171.9° and a torsion angle between the two hydrogen bonds of 88.0°. Its C_2 symmetry agrees with recent experimental Fourier transform infrared spectroscopy assignments based on isotope substitution studies in argon matrices (*8*). A second isomer, vinylidenecarbene, H_2CCC, has C_{2v} symmetry and lies 134.9 kJ mol^{-1} above propargylene. Its enthalpy of formation ΔH_f° (0 K) = 678.6 kJ mol^{-1} is in excellent agreement with an experimen-

Department of Chemistry, University of California, Berkeley, CA 94720, USA, and Chemical Sciences Division, Lawrence Berkeley National Laboratory, Berkeley, CA 94720, USA.